

# Reduced threshold current density of GaN-based green laser diode by applying polarization doping $p$ -cladding layer

Lingrong Jiang (江灵荣)<sup>1,2,3</sup>, Jianping Liu (刘建平)<sup>1,2,3\*</sup>, Lei Hu (胡磊)<sup>1,2,3</sup>, Liqun Zhang (张立群)<sup>1,3</sup>, Aiqin Tian (田爱琴)<sup>1,3</sup>, Wei Xiong (熊巍)<sup>1,3,4</sup>, Xiaoyu Ren (任霄钰)<sup>1,3</sup>, Siyi Huang (黄思溢)<sup>1,2,3</sup>, Wei Zhou (周伟)<sup>1,3</sup>, Masao Ikeda (池田昌夫)<sup>1,3</sup>, and Hui Yang (杨辉)<sup>1,2,3</sup>

<sup>1</sup>Suzhou Institute of Nano-tech and Nano-bionics, Chinese Academy of Sciences, Suzhou 215123, China

<sup>2</sup>School of Nano-tech and Nano-bionics, University of Science and Technology of China, Hefei 230026, China

<sup>3</sup>Key Laboratory of Nanodevices and Applications, Chinese Academy of Sciences, Suzhou 215123, China

<sup>4</sup>Nano Science and Technology Institute, University of Science and Technology of China, Hefei 230026, China

\*Corresponding author: [jpliu2010@sinano.ac.cn](mailto:jpliu2010@sinano.ac.cn)

Received April 20, 2021 | Accepted June 7, 2021 | Posted Online September 18, 2021

Absorption induced by activated magnesium (Mg) in a  $p$ -type layer contributes considerable optical internal loss in GaN-based laser diodes (LDs). An LD structure with a distributed polarization doping (DPD)  $p$ -cladding layer (CL) without intentional Mg doping was designed and fabricated. The influence of the anti-waveguide structure on optical confinement was studied by optical simulation. The threshold current density, slope efficiency of LDs with DPD  $p$ -CL, and Mg-doped CL, respectively, were compared. It was found that LDs with DPD  $p$ -CL showed lower threshold current density but reduced slope efficiency, which were caused by decreasing internal loss and hole injection, respectively.

**Keywords:** polarization doping; internal loss; GaN; laser diode.

**DOI:** [10.3788/COL202119.121404](https://doi.org/10.3788/COL202119.121404)

## 1. Introduction

Visible laser diodes (LDs) based on group III nitride materials have been employed as light sources in many fields such as full-color laser projection, laser lighting, under water communication, and material processing<sup>[1-5]</sup>. Despite their considerable commercial success in some areas, great efforts to further decrease threshold current density and to increase slope efficiency of LDs are needed to meet wider application requirements<sup>[6]</sup>. One of the obstacles hindering progress is the large optical internal loss, including absorption in  $p$ -doped layers, absorption by the passive regions, re-absorption of quantum wells (QWs), and absorption and scattering related to chip processing. It is believed that optical absorption loss caused by impurity doping, especially magnesium (Mg) doping, is the main source of internal loss<sup>[7-9]</sup>. Kioupakis *et al.* reported that acceptor-bound hole absorption was the dominant mechanism by theoretical calculation<sup>[8]</sup>. For the conventional structure of GaN-based LDs, Mg-doped AlGaIn is applied as the electron blocking layer (EBL) and  $p$ -cladding layer ( $p$ -CL). These heavily doped layers have a large overlap with the modal optical field. Optical loss caused by Mg doping in visible LDs is

approximately  $10 - 15 \text{ cm}^{-1}$  based on the absorption coefficient data given by Sizov *et al.*<sup>[9]</sup>, while the typical internal loss of the LDs is about  $15 - 30 \text{ cm}^{-1}$ , which means a majority of internal loss originates from the Mg doping layer. Thus, the performance improvements of visible LDs are limited by Mg doping induced internal loss. Decreasing the internal loss can be achieved by reducing the overlap of the waveguide mode with a Mg-doped layer, specifically, shifting the optical field away from the doped layer or decreasing the doping concentration. The movement of the optical field to the  $n$ -side may have detrimental impacts on the optical confinement factor of QWs and mode confinement, therefore leading to lower mode gain and a stronger substrate mode<sup>[10]</sup>, respectively. Decreasing the Mg doping concentration directly will increase electrical resistance of the  $p$ -type layer because of the low ionization rate of Mg in nitride materials, which can increase forward voltage and decrease injection efficiency.

Distributed polarization doping (DPD) is a newly proposed technique that can provide holes in nitride materials without Mg doping<sup>[11,12]</sup>; therefore, it is possible to reduce internal loss by suppressing the Mg doping concentration in  $p$ -CL and maintain enough hole concentration at the same time. Currently, the

applications on DPD focus on  $p$ -CL in ultraviolet (UV) devices and show some inspirational results<sup>[13–16]</sup>. However, decreasing internal loss by DPD in visible LDs has not been reported yet.

In this article, we designed and fabricated GaN-based green LDs with low threshold current density by employing DPD  $p$ -CL. Optical simulations and calculations were introduced to design and analyze the LDs. Device measurements showed the threshold current density of green LDs was reduced by half (from 3.15 kA/cm<sup>2</sup> to 1.7 kA/cm<sup>2</sup>), while the slope efficiency deteriorated. The possible reason for these changes has been explored.

## 2. Experimental Details

Two LD structures (named *Polar.* and *Ref.* LDs, respectively) were designed, as shown in Fig. 1(a). Low growth temperature and a hybrid  $p$ -CL layer were used to suppress the thermal budget to QWs during  $p$ -CL growth, which was demonstrated in our previous work<sup>[17–19]</sup>. The layer structure is the same for *Ref.* LDs and *Polar.* LDs except for the following part. For *Ref.* LDs, 300 nm Al<sub>0.035</sub>GaN  $p$ -CL with  $1 \times 10^{19}$  cm<sup>-3</sup> Mg doping and 20 nm Al<sub>0.2</sub>GaN EBL with  $1 \times 10^{19}$  cm<sup>-3</sup> Mg doping were adopted. For *Polar.* LDs, the EBL structure was removed, and  $p$ -CL consisted of 150 nm undoped AlGaIn with Al composition grading from 0.15 to 0.02 and 150 nm Al<sub>0.02</sub>GaN with  $1 \times 10^{19}$  cm<sup>-3</sup> Mg doping.

The theoretical hole concentration  $p$  in the DPD structure can be calculated as follows<sup>[20]</sup>:

$$\sigma = P_{\text{total}} = P_{\text{sp}}^{\text{AlGaIn}} + P_{\text{pz}}^{\text{AlGaIn}} - P_{\text{sp}}^{\text{GaN}}, \quad (1)$$

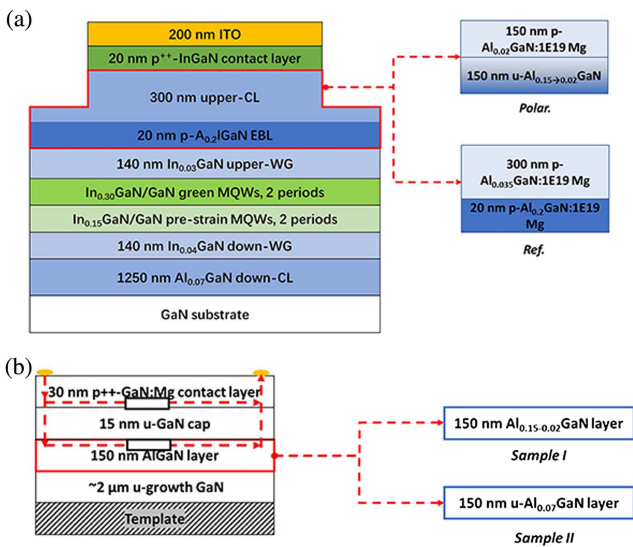


Fig. 1. (a) Schematic structures of green *Polar.* and *Ref.* LDs, respectively. (b) Sample structure for Hall measurements, the dash line shows the current pathway in measurement.

$$P_{\text{pz}}^{\text{AlGaIn}} = 2 \left( e_{31} - \frac{c_{13}}{c_{33}} e_{33} \right) \left( \frac{a_{\text{GaN}} - a_{\text{AlGaIn}}}{a_{\text{AlGaIn}}} \right), \quad (2)$$

$$p = \frac{\Delta\sigma}{q\Delta d}, \quad (3)$$

where  $\Delta\sigma$  is the deviation of net polarization charge densities in the graded layer,  $e$  is the piezoelectric constants,  $c$  is the elastic constants,  $a$  is the lattice constants,  $q$  is the elementary charge, and  $\Delta d$  is the layer thickness (in centimeters). Material parameters are taken from Refs. [21–23]. According to Eqs. (1)–(3), we can deduce that

$$p \approx 5.4 \times 10^{13} \cdot \frac{\Delta x}{\Delta d} \text{ cm}^{-3}, \quad (4)$$

where  $\Delta x$  is the Al composition variation. According to Eq. (4), the estimated hole concentration in the designed DPD layer of *Polar.* LDs is about  $4.7 \times 10^{17}$  cm<sup>-3</sup>. In order to obtain the actual hole concentration of the DPD layer, two samples for Hall measurements are designed, as shown in Fig. 1(b). For sample I, the measured sheet carrier density  $p_1$  ( $7.46 \times 10^{12}$  cm<sup>-2</sup>) consists of the sheet carrier density of the Al<sub>0.15–0.02</sub>GaN and GaN contact layers. For sample II, the measured sheet carrier density  $p_2$  ( $4.12 \times 10^{12}$  cm<sup>-2</sup>) originates from the GaN contact layer. Then, the net sheet carrier density of Al<sub>0.15–0.02</sub>GaN is  $p_3 = p_1 - p_2 = 3.34 \times 10^{12}$  cm<sup>-2</sup>. The hole concentration in Al<sub>0.15–0.02</sub>GaN can be calculated as  $p = p_3/d_{\text{AlGaIn}} = 2.23 \times 10^{17}$  cm<sup>-3</sup>, which is quite close to the one in conventional Mg doping AlGaIn used in *Ref.* LDs<sup>[18]</sup> and even smaller than the calculated value.

## 3. Results and Discussion

As the composition-graded layer in *Polar.* LDs will lead to the anti-waveguide structure, which may influence the optical confinement factor ( $\Gamma$ ) and substrate mode intensity, the distribution of the optical field was calculated by commercial optical simulation software named MODE SOLUTION developed by Lumerical Inc. More details on the optical simulations and refractive index data for nitride materials at the green wavelength range can be found in Ref. [10]. The simulation results are shown in Fig. 2. The optical confinement factors of QWs are 0.9143% for *Polar.* LDs and 0.9269% for *Ref.* LDs, respectively. The difference of  $\Gamma_{\text{2QWs}}$  is quite small, and thus it will not have obvious impacts on the threshold current density or slope efficiency. We can also find that the intensity of the substrate mode increases from  $2 \times 10^{-3}$  to  $1.2 \times 10^{-2}$ , which means LDs with DPD  $p$ -CL may suffer from more severe mode leakage. On the one hand, as the absolute value of the leaked mode and the absorption coefficient of the Si-doped layer are small, the increased substrate mode intensity will not have an obvious impact on LD output power and threshold current density. On the other hand, the enhanced leaked mode will have a negative impact on the far-field pattern of LDs. Both the variation of

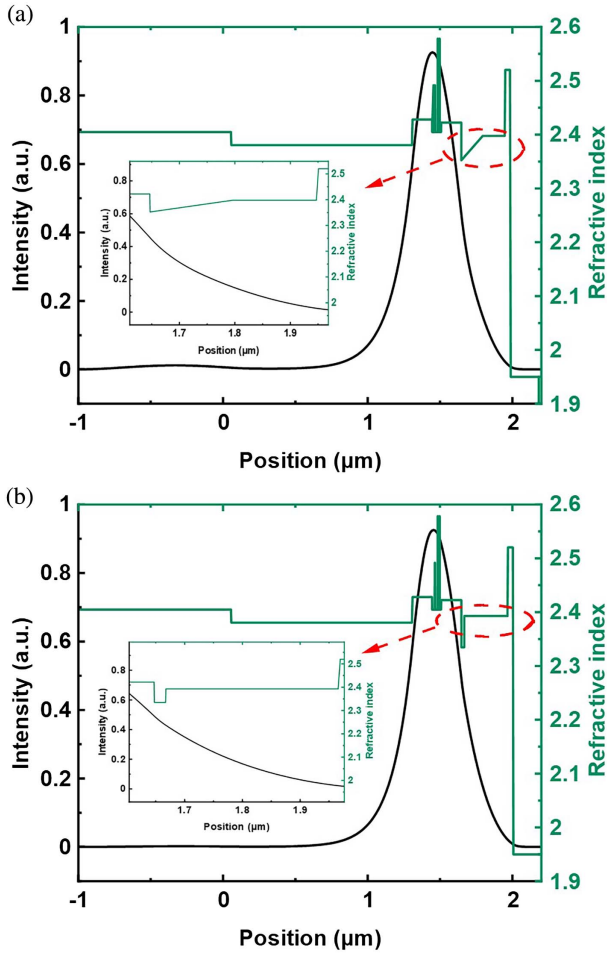


Fig. 2. Simulated optical field distribution of (a) LDs with DPD *p*-CL and (b) LDs with Mg doping *p*-CL. Insets show the enlarged distribution around *p*-CL.

$\Gamma_{2QWs}$  and substrate mode intensity can be explained by the prominent movement of the optical field to the *n*-side in *Polar.* LD as the result of higher average Al composition in the DPD layer.

*Polar.* and *Ref.* structures, respectively, were grown by metal organic chemical vapor deposition. Inductively coupled plasma dry etching was used to form the ridge waveguide LDs. A 200 nm Si dioxide layer was deposited as the insulating layer using inductively coupled plasma chemical vapor deposition on both sides of the ridges. A 200 nm indium tin oxide (ITO) layer was then deposited on top of the ridge using electron beam evaporation. About 100/500 nm of titanium (Ti)/Au was then deposited on top of ITO as a *p* pad and 50/100/50/100 nm of Ti/Al/Ti/Au was deposited on the backside of the wafer to form the *n* electrode. The LD cavity facets were formed by cleaving among the *m*-plane of the GaN crystal and then depositing dielectric films. Then, the ridge LDs were measured under pulse operation at room temperature, and the results are shown in Fig. 3(a). The structure of LDs was the same as the one described above, and the facet reflectivities were 95% and 70%, respectively. The size of the ridge was 15  $\mu\text{m} \times 1200 \mu\text{m}$ . As can be seen in Fig. 3(a), the threshold current density has been reduced obviously (from 3.15  $\text{kA}/\text{cm}^2$  to 1.7  $\text{kA}/\text{cm}^2$ ). However, the slope efficiency of *Polar.* LDs decreased greatly compared with that of *Ref.* LDs (0.07 W/A versus 0.35 W/A). Figure 3(b) shows the lasing spectra of these two LDs. The wavelength difference may be caused by composition variation in InGaN/GaN multi-QWs (MQWs) of these two samples.

Then, the reason for improved threshold current density and deteriorative slope efficiency was explored. According to Refs. [24,25], the threshold current density and slope efficiency of the LDs could be expressed as follows:

$$J_{th} = \frac{J_{tr}}{\eta_i \eta_{inj}} \cdot \exp\left(\frac{\alpha_i + \alpha_m}{\Gamma_{2QWs} g_0}\right), \quad (5)$$

$$S.E. = \frac{hc}{q\lambda} \cdot \frac{\alpha_m}{\alpha_m + \alpha_i} \cdot \eta_i \eta_{inj}, \quad (6)$$

$$\alpha_m = \frac{1}{2L} \ln\left(\frac{1}{R_1 R_2}\right), \quad (7)$$

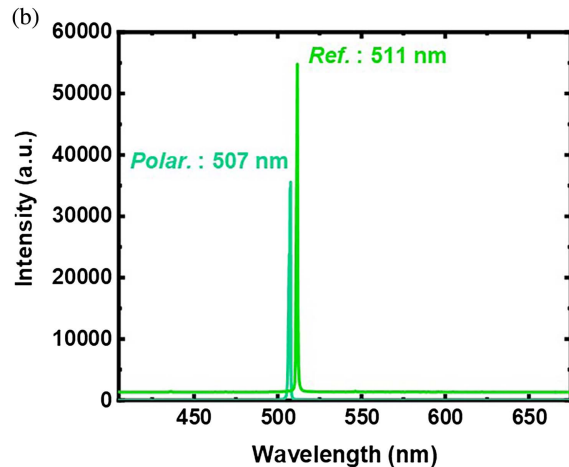
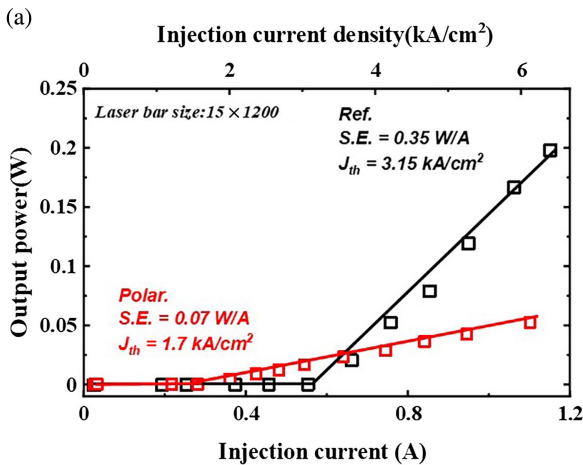


Fig. 3. (a) Power-current (*P-I*) curves and (b) laser spectra of green LDs with DPD and conventional Mg doping *p*-CL, respectively. The solid line in (a) is a guide for the eye.

where  $J_{tr}$ ,  $\eta_i$ ,  $\eta_{inj}$ ,  $\alpha_i$ ,  $L$ ,  $R$ ,  $g_0$ ,  $h$ ,  $c$ ,  $q$ , and  $\lambda$  are the transparent current density, internal quantum efficiency, injection efficiency, internal loss, cavity length ( $L = 1200 \mu\text{m}$ ), reflectivity of facet, material gain coefficients, Planck constant, speed of light, electron charge, and wavelength of light, respectively. The transparent current density was assumed to be  $0.4 \text{ kA/cm}^2$ , which is higher than the reported one for blue LDs<sup>[26]</sup>. The values of injection efficiency and internal quantum efficiency were 90% and 75%, respectively, based on the measurements of our LDs. The material gain was set as  $660 \text{ cm}^{-1}$  according to our measurements and this value is close to the one demonstrated by Ref. [27]. For the absorption in  $p$ -doped,  $n$ -doped, and ITO layers, we assumed absorption coefficients  $\alpha_0$  of  $50 \text{ cm}^{-1}$ ,  $10 \text{ cm}^{-1}$ <sup>[28]</sup>, and  $2000 \text{ cm}^{-1}$ <sup>[19]</sup>, respectively. Then, the total internal loss can be calculated by

$$\alpha_i = \sum \Gamma \cdot \alpha_0. \quad (8)$$

Applying Eq. (8), the total internal loss in *Polar.* and *Ref.* LDs was  $4.67 \text{ cm}^{-1}$  and  $9.57 \text{ cm}^{-1}$ , respectively. It should be pointed out that only 150 nm conventional Mg doping  $p$ -CL near the QW side had been replaced by the DPD layer, and EBL had been removed, but the internal loss of *Polar.* LDs was almost 50% smaller than that of the *Ref.* LDs. These results can be well understood by the significant suppression of the overlap of the optical field and Mg doping layer. This indicated the great potential of DPD in decreasing internal loss in nitride LDs. Thus, the threshold current density and slope efficiency can be calculated by Eqs. (5)–(7):  $1.67 \text{ kA/cm}^2$  and  $0.43 \text{ W/A}$  for *Polar.* LDs,  $3.71 \text{ kA/cm}^2$  and  $0.25 \text{ W/A}$  for *Ref.* LDs, respectively. The predicted 50% reduction in threshold current density agrees well with the measurement results.

Since we have confirmed *Polar.* LDs have smaller internal loss, it is reasonable to speculate that the decreasing injection efficiency is the reason for deteriorative slope efficiency according to Eq. (6). Figure 4 shows the temperature dependent photoluminescence (TDPL) result of *Polar.* LDs, which indicates that the internal quantum efficiency is 50%. Thus, the injection efficiency is 22%. This value is pretty low compared with the estimated one in the calculations (90%). Actually, GaN-based LDs with DPD  $p$ -CL show that very low injection efficiency have also been demonstrated in UV-C devices<sup>[29]</sup>, although, in theory, DPD  $p$ -CL is expected to provide relatively high hole concentration without Mg doping<sup>[30]</sup>. It is worth noting that Hall measurements based on the Van der Pauw method are usually applied to extract the carrier information of a single layer. However, the information given by this method corresponds to horizontal transportation in the films, which is different from the situation in actual devices (carrier transport in vertical direction). Thus, even though we can obtain relatively good conductivity (high hole concentration and mobility) for single layers, the hole injection in the vertical direction may be a problem. Figure 5 presents the  $I$ - $V$  curves of *Polar.* and *Ref.* LDs. It can be seen that the turn-on voltage of *Polar.* LDs is 6 V, which is about 2 V higher than that of the *Ref.* LDs. The higher turn-

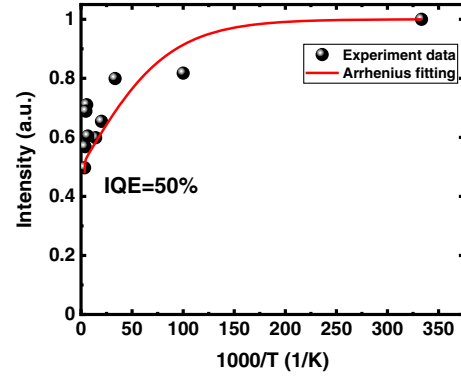


Fig. 4. TDPL result of *Polar.* LD. The solid line is the result of Arrhenius fitting.

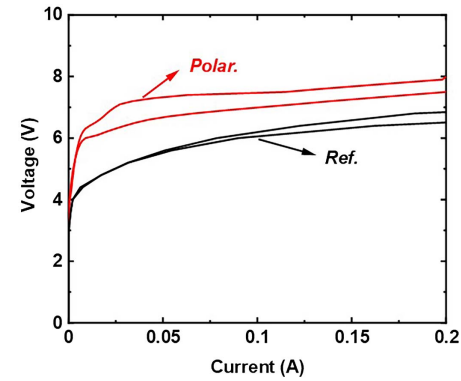


Fig. 5. Current-voltage ( $I$ - $V$ ) curves of green LDs with DPD and Mg doping  $p$ -CL, respectively.

on voltage suggests that there are potential barriers in *Polar.* LDs.

The cause for low injection efficiency has not been figured out yet, and some suppositions have been given in literatures. The consumption induced by point defects in Al-rich AlGaN had been attributed to one of the reasons in UV LDs<sup>[29]</sup>. However, considering the average Al composition is only about 8% for our samples, which is far less than that in UV devices, the material quality should not be the main problem. Another possible reason may be the carrier spillover. Sato *et al.* demonstrated that UV-B LDs with DPD  $p$ -CL had spontaneous subpeak emission, which could consume injected carriers by recombination at the potential minimum formed at the interface of the waveguide layer (WG) and EBL because of large polarization discontinuity<sup>[31]</sup>. Unfortunately, this interpretation cannot explain our cases, as the polarization discontinuity between WG and EBL (acted by the DPD  $p$ -CL because the Al composition near the WG is as large as 15%) in the *Polar.* LD is even smaller than that in the *Ref.* LD since the Al composition is smaller (15% versus 20%), and we also did not observe any subpeak in the photoluminescence measurement, as shown in Fig. 3(b). Reference [32] demonstrated that blue LEDs with DPD EBL showed higher turn-on voltage and lower injection efficiency compared with the reference samples, although high hole concentration in a



composition-graded AlGaIn had been observed clearly by separate Hall measurement<sup>[20]</sup>. It is believed that polarization charges at the interface can induce dips or spikes in energy band profiles, hindering holes injection. Then, the polarization doping concept was proposed, while the performances of LEDs with DPD are still inferior to the references at low injection currents. Since DPD is realized by inducing high concentration net negative polarization charges in film to attract holes, those fixed charges may have a detrimental effect on the carrier transportation, which needs further study to confirm. It is worth pointing out that the hole concentration for our structure is  $2.23 \times 10^{17} \text{ cm}^{-3}$ , which can be increased by applying larger Al composition. The increased hole concentration is helpful to improve hole injection.

#### 4. Conclusions

GaN-based green LDs with DPD and Mg doping *p*-CL, respectively, were designed and fabricated. LDs with DPD *p*-CL showed reduced threshold current density but lower slope efficiency. Reduction of internal loss by DPD is the main reason for decreasing the threshold current density. The low slope efficiency is attributed to small low injection efficiency, which may be caused by poor hole transportation in the vertical direction. This research proves the possibility to decrease threshold current density by DPD, while further work to improve hole injection is needed.

#### Acknowledgement

This work was supported by the National Natural Science Foundation of China (Nos. 61834008, 61574160, 61804164, and 61704184), National Key Research and Development Program of China (Nos. 2017YFE0131500 and 2017YFB0405000), Natural Science Foundation of Jiangsu Province (No. BK20180254), and China Postdoctoral Science Foundation (No. 2018M630619).

#### References

- H. Wang, Y. Kawahito, R. Yoshida, Y. Nakashima, and K. Shiokawa, "Development of a high-power blue laser (445 nm) for material processing," *Opt. Lett.* **42**, 2251 (2017).
- S. Nagahara, "Three primary color LD module," *SID Symp. Digest Tech. Papers* **48**, 80 (2017).
- X. Liu, S. Yi, X. Zhou, Z. Fang, Z.-J. Qiu, L. Hu, C. Cong, L. Zheng, R. Liu, and P. Tian, "34.5 m underwater optical wireless communication with 2.70 Gbps data rate based on a green laser diode with NRZ-OOK modulation," *Opt. Express* **25**, 27937 (2017).
- X. Huang, F. Yang, and J. Song, "Hybrid LD and LED-based underwater optical communication: state-of-the-art, opportunities, challenges, and trends," *Chin. Opt. Lett.* **17**, 100002 (2019).
- L.-K. Chen, Y. Shao, and R. Deng, "Robust UOWC systems against bubble-induced impairments via transmit/receive diversities," *Chin. Opt. Lett.* **17**, 100006 (2019).
- H. König, M. Ali, W. Bergbauer, J. Brückner, G. Brüderl, C. Eichler, S. Gerhard, U. Heine, A. Lell, L. Naehle, M. Peter, J. Ristic, G. Rossbach, A. Somers, B. Stojetz, S. Tautz, J. Wagner, T. Wurm, U. Strauss, M. Baumann, A. Balck, and V. Krause, "Visible GaN laser diodes: from lowest thresholds to highest power levels," *Proc. SPIE* **10939**, 109390C (2019).
- E. Kioupakis, P. Rinke, and C. G. Van de Walle, "Determination of internal loss in nitride lasers from first principles," *Appl. Phys. Express* **3**, 082101 (2010).
- E. Kioupakis, P. Rinke, A. Schleife, F. Bechstedt, and C. G. Van de Walle, "Free-carrier absorption in nitrides from first principles," *Phys. Rev. B* **81**, 241201 (2010).
- D. Sizov, R. Bhat, and C.-E. Zah, "Optical absorption of Mg-doped layers and InGaIn quantum wells on *c*-plane and semipolar GaN structures," *J. Appl. Phys.* **113**, 203108 (2013).
- L. Jiang, J. Liu, L. Zhang, B. Qiu, A. Tian, L. Hu, D. Li, S. Huang, W. Zhou, M. Ikeda, and H. Yang, "Suppression of substrate mode in GaN-based green laser diodes," *Opt. Express* **28**, 15497 (2020).
- J. Simon, V. Protasenko, C. Lian, H. Xing, and D. Jena, "Polarization-induced hole doping in wide-band-gap uniaxial semiconductor heterostructures," *Science* **327**, 60 (2010).
- S. Li, M. E. Ware, J. Wu, V. P. Kunets, M. Hawkrige, P. Minor, Z. Wang, Z. Wu, Y. Jiang, and G. J. Salamo, "Polarization doping: reservoir effects of the substrate in AlGaIn graded layers," *J. Appl. Phys.* **112**, 053711 (2012).
- O. V. Khokhlev, K. A. Bulashevich, and S. Y. Karpov, "Polarization doping for III-nitride optoelectronics," *Phys. Status Solidi A* **210**, 1369 (2013).
- Z. Zhang, M. Kushimoto, T. Sakai, N. Sugiyama, L. J. Schowalter, C. Sasaoka, and H. Amano, "A 271.8 nm deep-ultraviolet laser diode for room temperature operation," *Appl. Phys. Express* **12**, 124003 (2019).
- K. Sato, S. Yasue, Y. Ogino, S. Tanaka, M. Iwaya, T. Takeuchi, S. Kamiyama, and I. Akasaki, "Light confinement and high current density in UVB laser diode structure using Al composition-graded *p*-AlGaIn cladding layer," *Appl. Phys. Lett.* **114**, 191103 (2019).
- D. Zhao, "III-nitride based ultraviolet laser diodes," *J. Semicond.* **40**, 120402 (2019).
- Z. Li, J. Liu, M. Feng, K. Zhou, S. Zhang, H. Wang, D. Li, L. Zhang, D. Zhao, D. Jiang, H. Wang, and H. Yang, "Suppression of thermal degradation of InGaIn/GaN quantum wells in green laser diode structures during the epitaxial growth," *Appl. Phys. Lett.* **103**, 152109 (2013).
- A. Tian, J. Liu, M. Ikeda, S. Zhang, Z. Li, M. Feng, K. Zhou, D. Li, L. Zhang, P. Wen, F. Zhang, and H. Yang, "Conductivity enhancement in AlGaIn:Mg by suppressing the incorporation of carbon impurity," *Appl. Phys. Express* **8**, 051001 (2015).
- L. Hu, X. Ren, J. Liu, A. Tian, L. Jiang, S. Huang, W. Zhou, L. Zhang, and H. Yang, "High-power hybrid GaN-based green laser diodes with ITO cladding layer," *Photon. Res.* **8**, 279 (2020).
- T. Yasuda, K. Yagi, T. Suzuki, T. Nakashima, M. Watanabe, T. Takeuchi, M. Iwaya, S. Kamiyama, and I. Akasaki, "Investigations of polarization-induced hole accumulations and vertical hole conduction in GaN/AlGaIn heterostructures," *Jpn. J. Appl. Phys.* **52**, 08J05 (2013).
- F. Bernardini, V. Fiorentini, and D. Vanderbilt, "Spontaneous polarization and piezoelectric constants of III-V nitrides," *Phys. Rev. B* **56**, R10024 (1997).
- M. Asif Khan, A. Bhattarai, J. N. Kuznia, and D. T. Olson, "High electron mobility transistor based on a GaN-Al<sub>x</sub>Ga<sub>1-x</sub>N heterojunction," *Appl. Phys. Lett.* **63**, 1214 (1993).
- K. Kim, W. R. L. Lambrecht, and B. Segall, "Elastic constants and related properties of tetrahedrally bonded BN, AlN, GaN, and InN," *Phys. Rev. B* **53**, 16310 (1996).
- L. A. Coldren, S. W. Corzine, and M. L. Mašanović, "A phenomenological approach to diode lasers," in *Diode Lasers and Photonic Integrated Circuits*, 2nd ed. (Wiley, 2012).
- M. Kawaguchi, O. Imafuji, S. Nozaki, H. Hagino, S. Takigawa, T. Katayama, and T. Tanaka, "Optical-loss suppressed InGaIn laser diodes using undoped thick waveguide structure," *Proc. SPIE* **9748**, 974818 (2016).
- H. Y. Ryu, K. H. Ha, J. K. Son, S. N. Lee, H. S. Paek, T. Jang, Y. J. Sung, K. S. Kim, H. K. Kim, Y. Park, and O. H. Nam, "Determination of internal parameters in blue InGaIn laser diodes by the measurement of cavity-length dependent characteristics," *Appl. Phys. Lett.* **93**, 011105 (2008).
- D. J. Kunzmann, R. Kohlstedt, T. Uhlig, and U. T. Schwarz, "Critical discussion of the determination of internal losses in state-of-the-art (Al, In)GaIn laser diodes," *Proc. SPIE* **11280**, 112800Y (2020).
- M. Kuramoto, C. Sasaoka, N. Futagawa, M. Nido, and A. A. Yamaguchi, "Reduction of internal loss and threshold current in a laser diode with a

- ridge by selective re-growth (RiS-LD),” *Phys. Status Solidi A* **192**, 329 (2002).
29. Z. Zhang, M. Kushimoto, T. Sakai, N. Sugiyama, L. J. Schowalter, C. Sasaoka, and H. Amano, “Design and characterization of a low-optical-loss UV-C laser diode,” *Jpn. J. Appl. Phys.* **59**, 094001 (2020).
30. Z. Zhang, M. Kushimoto, M. Horita, N. Sugiyama, L. J. Schowalter, C. Sasaoka, and H. Amano, “Space charge profile study of AlGaIn-based p-type distributed polarization doped claddings without impurity doping for UV-C laser diodes,” *Appl. Phys. Lett.* **117**, 152104 (2020).
31. K. Sato, S. Yasue, Y. Ogino, M. Iwaya, T. Takeuchi, S. Kamiyama, and I. Akasaki, “Analysis of spontaneous subpeak emission from the guide layers of the ultraviolet-B laser diode structure containing composition-graded p-AlGaIn cladding layers,” *Phys. Status Solidi A* **217**, 1900864 (2020).
32. T. Yasuda, K. Hayashi, S. Katsuno, T. Takeuchi, S. Kamiyama, M. Iwaya, I. Akasaki, and H. Amano, “Polarization dilution in a Ga-polar UV-LED to reduce the influence of polarization charges,” *Phys. Status Solidi A* **212**, 920 (2015).